Evolution and cleaning of the deposit layers on the lower divertor of WEST fully equipped with ITER grade components

J. Gerardin, Y. Corre, C. Desgranges, M. Diez, L. Dubus, M. Firdaouss, J. Gaspar, A. Grosjean, C. Guillemaut, C. Hernandez, et al.

Nuclear Materials and Energy 41 (2024) 101783

Contents lists available at ScienceDirect

Nuclear Materials and Energy

journal homepage: www.elsevier.com/locate/nme

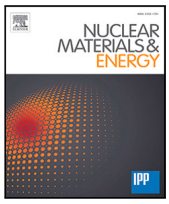

Evolution and cleaning of the deposit layers on the lower divertor of WEST fully equipped with ITER grade components

J. Gerardin [a,*], Y. Corre [a], C. Desgranges [a], M. Diez [a], L. Dubus [a], M. Firdaouss [a], J. Gaspar [b], A. Grosjean [c], C. Guillemaut [a], C. Hernandez [a], A. Huart [a], H. Roche [a], S. Vives [a], WEST team

[a] CEA, IRFM, F-13108, Saint-Paul-lez-Durance, France
[b] IUSTI, Aix Marseille University, CNRS, Marseille, France
[c] Department of Nuclear Engineering, Knoxville, TN 37996, USA

ARTICLE INFO

Keywords:
ITER-grade W monoblock
Erosion-redeposition
Deposit
Cleaning
WEST

ABSTRACT

After 3 h of accumulated time from repeated plasma shots during C7 campaign performed in 2023, a deposited layer appeared on the ITER-grade W-monoblock of the lower divertor of WEST, mostly on the high field side. The growth of the deposit was observed during the campaign using infrared cameras, showing a large increase of the area covered by the deposit (x4) in the last two hours of cumulated plasma time. The deposit becomes problematic for the operation as it generates flakes which provoke radiative collapse when entering the plasma. A cleaning of the lower divertor is mandatory. A first cleaning was done using adhesive tape to remove all weakly adhered parts of the deposit. This method was chosen because it was easy to implement and did not generate dusts inside the tokamak. The cleaning enables partial removal of the more lightly adhered deposits but a large fraction remains stuck on the monoblock. A second cleaning was tried during 2024 operation by using the plasma as cleaner. A scenario was developed to put the inner strike line directly on the deposit to heat it and try to remove it by thermal stress. The deposit reaches temperature up to 1560° C but was not removed. The impurities generated were higher than normal operation and decreased during the cleaning session (−50% of light impurities observed at the end of the cleaning discharge session), showing an effect of cleaning by removing impurities from the deposit.

1. Introduction

The plasma facing components (PFCs) inside tokamaks have to sustain high heat and particles fluxes. The plasma erodes the PFCs, leading to damage of the PFCs and pollution of the plasma by the eroded material. The PFC conditions for ITER are to withstand a lifetime of 10 years and maintain their heat exhaust capabilities to ensure the repeatability of the high performance operation. WEST is a medium size tokamak which aims to test the tungsten (W) ITER-grade divertor monoblocks (MB) under relevant plasma conditions. The WEST lower divertor is equipped with 456 PFCs of 35 MB each. The MBs present a toroidal bevel on the top face of 0.5 mm height in order to protect the leading edge of the neighboring PFC. The full description of the WEST lower divertor with its shaping is done in [1]. To study the lifetime of the PFCs, a deuterium high-fluence campaign was carried out on WEST [2], during the C7 campaign in 2023, for one month, with attached plasma condition ($T_e \equiv 25$ eV), repeating the same shot 384 times for a total cumulated duration of 3 h of plasma. The campaign successfully cumulates particle flux comparable to two Pre Fusion Power Operation (PFPO) [3] ITER pulses. From this high fluence campaign, a deposited layer appeared on the High Field Side (HFS) of the lower divertor (see Fig. 1). This deposited layer is mainly made of W and W oxide [4]. The deposited layer is heterogeneous because of the toroidal bevel, with thinner weakly stuck deposit on the leading edges in the magnetically shadowed regions and thicker well stuck deposit in the wetted area of the lower divertor. This type of deposit was already found on JET [5] and Tore Supra [6]. It creates problems during operation when flakes (called Unknown Flying Objects UFOs) detached and entered the plasma. This leads to increased radiative power and could provoke a radiative collapse of the plasma. The number of discharges lost due to these UFOs was increasing during the C7 campaign [7]. In the first part of this paper, the evolution of the deposited layers, monitored with the infrared (IR) view [8], will be presented, showing the growth evolution during the C7 campaign. In the second part, the cleaning process tested during the shutdown, using

* Corresponding author.
E-mail address: jonathan.gerardin@cea.fr (J. Gerardin).
URL: https://irfm.cea.fr/en/west/WESTteam/ (W. team).

https://doi.org/10.1016/j.nme.2024.101783
Received 4 July 2024; Received in revised form 14 October 2024; Accepted 18 October 2024
Available online 26 October 2024

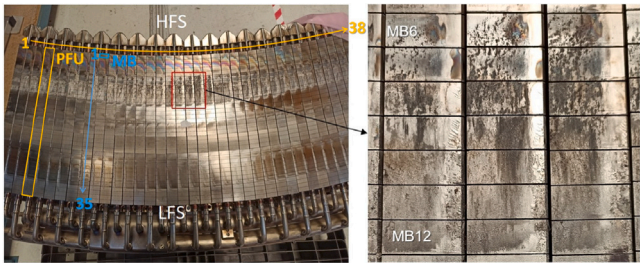

Fig. 1. Deposited layer observed on the HFS of the lower divertor after C7 experimental campaign.

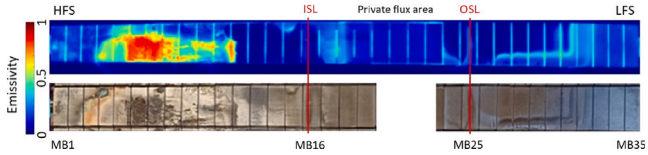

Fig. 2. Emissivity measured on the ITER-grade PFC after C7 experimental campaign and comparison with visual aspect of the PFC. (For interpretation of the references to color in this figure legend, the reader is referred to the web version of this article.)

adhesive tape, and its efficiency measured by confocal microscopy, is presented. The last part of the paper is dedicated to the experiment carried out during the C9 campaign (January 2024) in order to clean the deposit by the plasma, putting the inner strike line (ISL) directly on the deposit. Efficiency of the cleaning as measured by IR thermography and impurities measured by visible and extreme ultra violet (EUV) spectroscopy will be discussed.

2. InfraRed analysis of the deposit

2.1. Deposit observation with InfraRed camera

The deposit is visible on the IR camera for two main reasons.

Firstly, the deposit has higher rugosity which leads to higher emissivity. Emissivity measurement [9] performed on a PFC with deposit is shown in Fig. 2 and compared with the visual aspect of the PFC. One can see that the HFS deposit reaches emissivity above 0.4 and even between 0.8 to 1 on MB6-7, where the deposit visually appears the darkest. However, near the usual strike lines (ISL and outer strike line (OSL) represented by red lines on Fig. 2), the emissivity is 0.04 (close to the pure polished W surface), much lower than the emissivity in the private flux area (the area between the two usual strike lines) where the MBs are not touched by the plasma and keep the initial emissivity around 0.1–0.2. The higher emissivity of the deposit makes it more visible on the IR images.

Secondly, the deposit is not well attached to the lower divertor, the thermal contact is low and this implies a poor cooling of the deposit, compared to the bulk W monoblock [7,10]. The deposit will thus overheat and be more visible on the IR images compared to cleaned area with the same heat load.

Fig. 3 highlights the visual differences from apparent temperature between IR images at the beginning and the end of the C7 campaign, for two comparable plasma pulses. On the picture at the beginning of the C7 campaign, the strike lines are clearly visible with no signal on the HFS. At the end of the campaign, the strike lines are much less visible due to the loss of emissivity and the deposit area between MB6-12 on the HFS is clearly noticeable. The deposit is located 2 to 3 MBs away from the ISL.

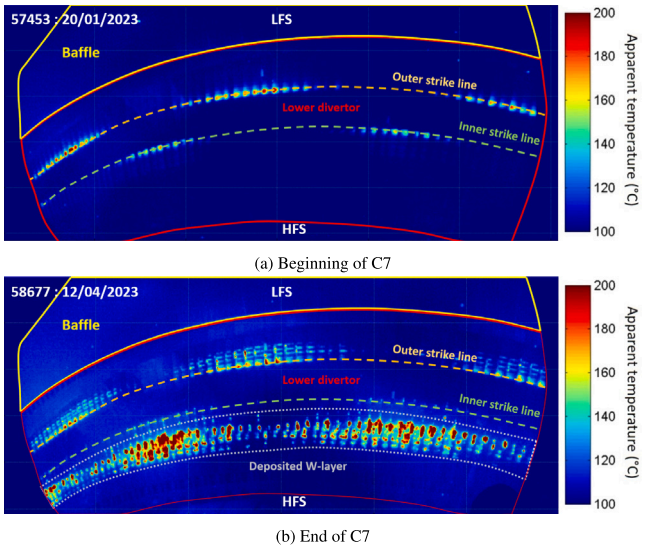

(a) Beginning of C7

(b) End of C7

Fig. 3. IR top view of the lower divertor at the beginning (top) and at the end (bottom) of the C7 experimental campaign.

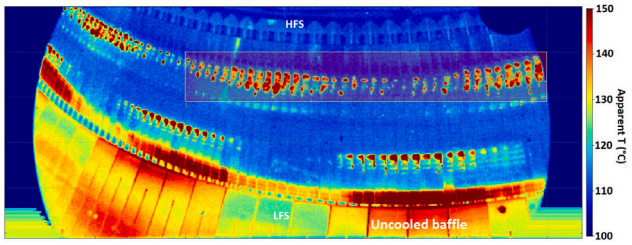

(a) IR image of the lower divertor (top view)

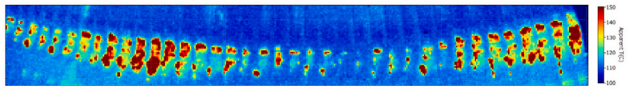

(b) Example of area used for growing analysis, covering 38 PFCs

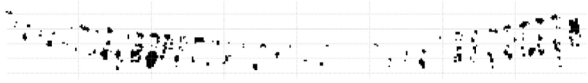

(c) Threshold on apparent temperature applied on the figure 4b. Black areas are above an apparent temperature of 150°C

Fig. 4. Methodology of the deposit IR analysis.

2.2. Growing of the deposit during high fluence campaign

To monitor the growing area of this W-deposit layer on the inner lower divertor, an analysis using the IR images (see Fig. 4(a)) was done during C7 campaign. A particular area on the inner lower divertor (see Fig. 4(b)) is monitored during the campaign and compared for similar shots (injected power, density, Ip current...). From this area, an apparent temperature threshold is applied and the number of pixels above the threshold are counted (see Fig. 4(c)).

On Fig. 5(a) is shown the evolution of the number of pixels above the temperature threshold for the area presented on Fig. 4(b) and for 4 different apparent temperature thresholds (from 150 °C to 225 °C) to investigate the sensitivity of the technique. The total area is made of 22 000 pixels. With apparent temperature threshold of 150 °C, a maximum of 3187 pixels reaches the temperature threshold (representing 14.4% area coverage), while with apparent temperature threshold of 225 °C, a maximum of 719 pixels only can reach this apparent temperature (3.2% area coverage). The choice of the temperature threshold has

thus a strong effect on the number of pixels detected. On Fig. 5(b), each curve was normalized according to their respective highest number of pixels. When the curve reaches 1, it means that it gets the highest surface coverage for the defined apparent temperature (and not that all pixels are above the threshold). One can see that the largest area coverage is obtained at the same time for all apparent temperatures, with relatively similar temporal evolution whatever the temperature chosen. After this normalization, the effect of the temperature threshold is much less visible, only the smallest temperature showed higher sensitivity after 2–3 h of plasma. For the first two hours of plasma during the campaign, no particular evolution was seen on the inner lower divertor. A small decrease is observed at the very beginning, some isolated PFUs had higher temperature probably due to higher roughness on top surface of the W MB (involving higher emissivity) and after some plasma discharges, they were polished, involving smaller emissivity. After 2 h of plasma, some evolution could be seen with the smallest temperature threshold. The deposit was still very thin at this moment, due to the large diversity of magnetic equilibria performed during the first phase of the campaign, distributing the deposit and thus not allowing its thickness to increase. The high fluence campaign started after having done 2.5 h of plasma. For the first hour of the high fluence campaign, the IR images were not showing a particular area increase of the deposit, the fluctuations observed for the smallest threshold temperature could be related to some fluctuations in the ambiant temperature inside the machine (as some components are not actively cooled, shots performed at the end of days have a surrounding temperature higher than shots from the beginning of the day) making some pixels passing above the temperature threshold and are not necessarily due to an evolution of the deposit. It needed thus 1 h of repeated plasma to cumulate enough deposit on the same location of the lower divertor to be really seen on IR view. But during the last two hours of plasma, the number of pixels above the threshold temperature increased suddenly to reach 10%–30% of maximum area, then increased globally linearly to reach 70% of the maximum area and finished with a strong increase (from 70% to 100% of maximum area) on the last 7 cumulated minutes of plasma. Moreover, the deposit area never stabilized, it was still increasing during the campaign, by spreading on new MBs but also by increasing the thickness of deposit (which increase its temperature due to the bad thermal contact). Even if the result from 1 standard divertor IR view was presented here, the same evolution was observed for all HFS areas on the 8 other standard divertor IR views of WEST. Some small decreases were observed at some moments during the campaign, which can be related to several consecutive shots which generates flakes, killing the discharge by a disruption on the lower divertor, generating new flakes from the deposit. If one of these flakes remain on the top surface of the lower divertor, it could go in the plasma during the next discharge, leading to a new disruption if its size was large enough (this phenomenon represented 27% of discharged killed by UFO [7]).

3. Cleaning of the lower divertor

3.1. Method

The cleaning of the lower divertor was performed by using adhesive tape (Honeywell Delta 300®). This method was chosen because it can be easily implemented during shutdown without dismounting the divertor or generating dust inside the tokamak. The procedure was to apply the adhesive tape on the deposit, ensuring a good contact and remove the adhesive tape. This process was repeated three times for each MB. All weakly adhered parts of deposit were clearly visible on the adhesive tape, showing less and less deposit after each cleaning. It needed two days of operation for three workers, using 250 m of adhesive tape. 9 PFCs of the more than 456 PFCs on the lower divertor were not cleaned in order to survey the behavior of these deposits in the next campaign.

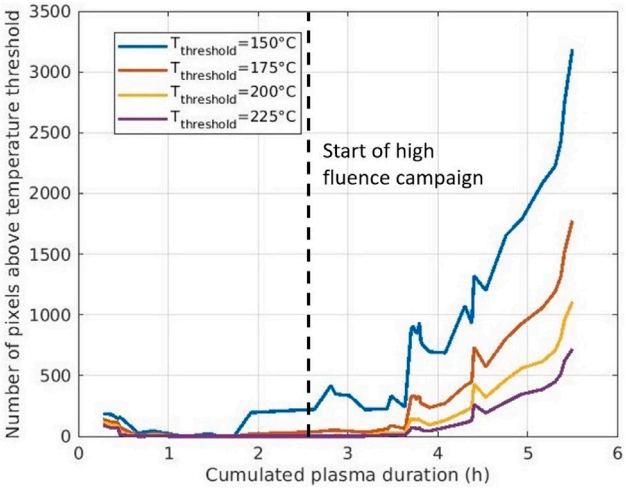

(a) Number of pixels above apparent temperature threshold

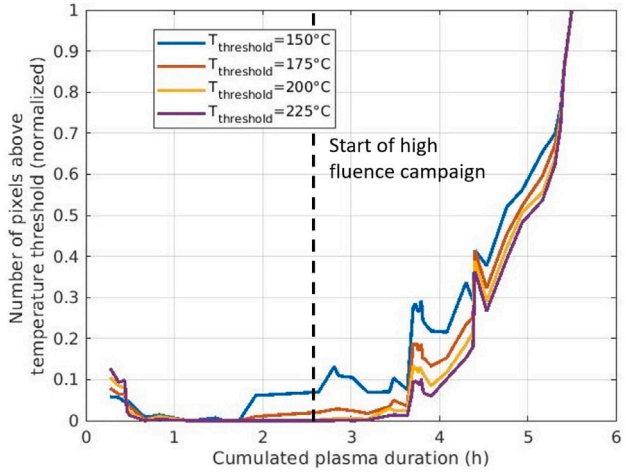

(b) Normalization to the maximum number of pixels

Fig. 5. Evolution of the deposit area during C7, by IR analysis, as function of cumulated plasma time.

3.2. Analysis of the cleaning

On Fig. 6 is shown a cleaning test made on one post-mortem PFC in the laboratory prior to in-situ cleaning. The adhesive tape was stuck on two pairs of MBs, one on MB6-7 and the other on MB9-10. The deposit removed by the adhesive tape is shown on the right of Fig. 6. A smaller part of deposit was removed on MB6-7, compared to MB9-10, where a large part of the deposit on the right of the MB was removed. As the deposit are thicker on MB9-10, it is expected to remove more deposit on them. The magnetic configuration inside the machine made the magnetic field line coming from the right to the left of these MBs, so the removed deposit part was in the shadow of the neighboring PFC (due to the bevel) and not directly touched by the plasma. All the parts on the left of the MBs are wetted by the plasma. On Fig. 7, one can see the effect of the cleaning by visual comparison between the left picture (before cleaning) and the right picture (after cleaning). The visual aspect is very similar in both cases. The only visual difference is on the bottom right part (in the red rectangle), where the MB appears darker after cleaning. This correspond to the part where a lot of deposit was stuck to the adhesive tape.

To quantify the thickness of deposit removed by usage of adhesive tape, confocal microscopy was performed on the PFC before and after cleaning. The confocal microscopy measures the depth of the deposits at different locations of the sample which can be used to create a 3-D

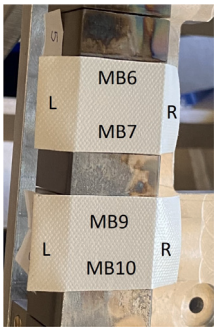

(a) Adhesive tape on the MBs

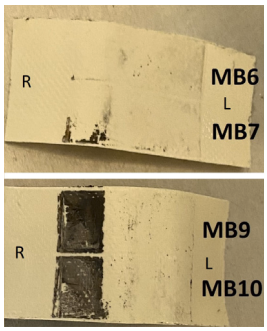

(b) Back side on the adhvesive tape with stuck deposit

Fig. 6. Test of cleaning of the lower divertor by using adhesive tape Honeywell Delta 300®.

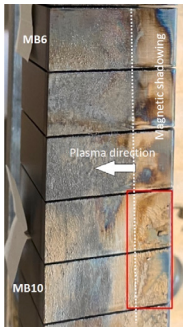

(a) Before cleaning

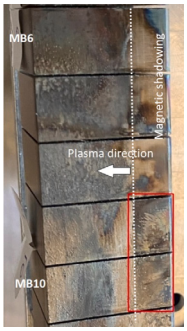

(b) After cleaning

Fig. 7. Visual comparison before and after cleaning by the adhesive tape. (For interpretation of the references to color in this figure legend, the reader is referred to the web version of this article.)

reconstruction. The accuracy in altitude is ±0.15 µm. For the current study, the lateral steps were 20 µm × 100 µm. On Fig. 8 is shown the 3D reconstruction of the PFC from the confocal microscopy. The PFC was measured before (left PFC) and after (right PFC) the cleaning with the adhesive tape. The thickness of the deposit (in Z direction) was amplified by a factor 10,000 to be visible. The roughness of the deposit is visible on the left part of the PFC and a strong deposit layer was measured on the right part of MB9. After the cleaning, the roughness on MB6-7 is slightly less visible and the strong deposit on MB9 is totally removed. To quantify the amount of deposit removed, profiles were plotted along the length of the PFC for all toroidal positions (direction Y). Profile along the magenta line is shown on Fig. 9(a), whereas profile along the green line is on Fig. 9(b). For the magenta profile, it is slightly visible that a small part of the deposit was removed by the adhesive, reducing the roughness of the MB6-7. But the height of deposit removed does not exceed 20 µm. On the contrary, the deposit located on the leading edge (actually, a partly detached deposit), with a height up to 240 µm, was totally removed by the adhesive.

The total volume removed can be computed by integrating the height from the different poloidal profiles (for each toroidal position in direction Y), assuming a constant profile over 100 µm between each poloidal profile (the toroidal distance between each poloidal profile measured by the confocal microscopy). The estimated volume of deposit extracted for the 4 MB is 4 mm^3. If distributed on a surface of 26 mm × 12 mm × 4 MB = 1248 mm^2, it gives an average removed deposit thickness of 3.2 µm.

4. Cleaning of the W-deposit by the plasma

A scenario was developed during C9 to try to clean the deposit with the plasma, as the cleaning by adhesive tape is less efficient on

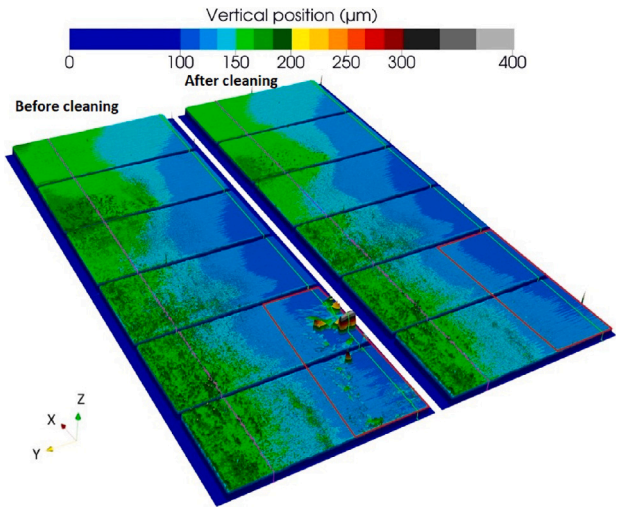

Fig. 8. Confocal microscopy comparison before and after cleaning. The height of the deposit (in Z direction) is amplified by factor 10,000. (For interpretation of the references to color in this figure legend, the reader is referred to the web version of this article.)

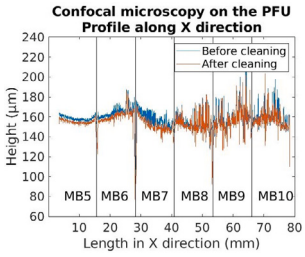

(a) Profile over magenta line of figure 8, area magnetically wetted by the plasma

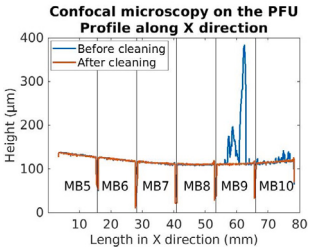

(b) Profile over green line of figure 8, area magnetically shadowed

Fig. 9. Profile on the confocal microscopy result at two different locations on the monoblock. (For interpretation of the references to color in this figure legend, the reader is referred to the web version of this article.)

the wetted area. The purpose is to put the ISL directly on the deposit to detach it by thermal stress. The experiment was performed at the beginning of C9, few weeks after the cleaning with the adhesive tape, to firstly be able to develop a magnetic configuration with ISL on the deposit. All weakly adhered parts of the deposit were thus already removed by the adhesive tape.

4.1. Experiments description

7 L-mode shots were successfully performed with the ISL on the deposit, for duration up to 40 s. Two other shots were lost due to UFOs. Plasma was heated using Lower Hybrid Current Drive antenna with 3.8 MW injected, leading to T_e around 20 eV on the target. Table 1 summarizes the different pulses done for cleaning with their main parameters (in gray). Two shots from other sessions (with similar plasma parameters but usual ISL position far from the deposit) are also mentioned for comparison. Different X-point heights (dX) were tested during the session to move the ISL on a larger area of the deposit. The strike points for each pulse are shown on Fig. 10 and localized on different radial position on MB11, either closer to MB12 or to MB10.

4.2. Infrared thermal analysis

On Fig. 11, the IR images from the Very High Resolution (VHR) camera [11], looking at a small part of the lower divertor (6MBs : 3MBs

Table 1
List of pulses during the cleaning experiment (gray) and pulses done before/after and used for comparison.

Date (2024)	Shot	ISL position	dX (mm)	IP (kA)	PLH (MW)
22/01	#59 037	MB16	60	380	2.8
26/01	#59 101	MB11	100	400	3.8
26/01	#59 102	MB11	100	400	3.8
26/01	#59 108	MB11	105	400	3.8
26/01	#59 109	MB11	110	400	3.8
26/01	#59 110	MB11	115	400	3.8
26/01	#59 115	MB11	120	400	3.8
26/01	#59 117	MB11	100	400	3.8
16/02	#59 438	MB16	60	400	3.6

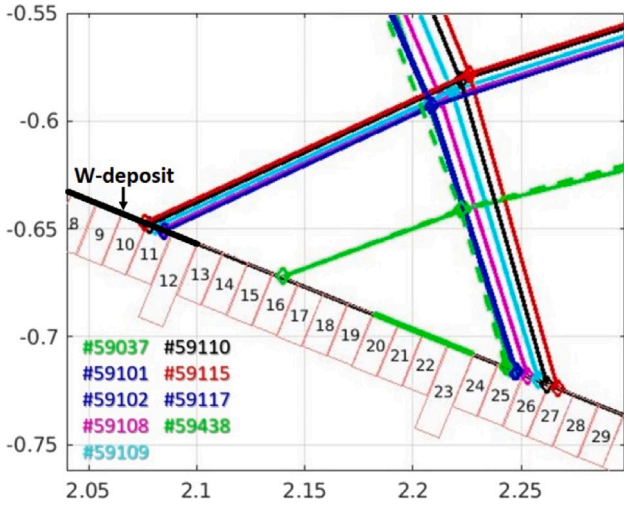

Fig. 10. Strike point position for the different shots performed during the cleaning experiment. The X-point position was increased to move the ISL toward HFS.

from 2 neighboring PFCs), is shown for two similar shots (#59 102 and #59 117) done during the session. The focus is particularly made on the PFC21 MB11 (see Fig. 1 for numbering of PFC and MB) of sector Q3B. This PFC was not cleaned with the adhesive tape so some weakly adhered parts of deposit could be removed. The deposit appears in red, much hotter than the bulk W monoblock, due to the emissivity and bad thermal contact and was heated up to 1400 °C in apparent temperature (assuming $\varepsilon = 1$), corresponding to 1563 °C with $\varepsilon = 0.8$, closer to the real emissivity of the deposit. A comparison of shot #59 102 and #59 117 (similar plasma parameters and ISL) is shown. The first shot was at the beginning of the session and the second one is at the end of the session. Several areas of deposits on the left picture are not appearing on the right picture, showing a slight modification of the deposit, with at least partial removal. However, the estimated area removed (by comparing pixels temperature of both shots and using a pixel size of 0.08 mm) remains smaller than 14 mm^2, which represents less than 5% of the MB surface.

4.3. Spectroscopy

4.3.1. Extreme UltraViolet spectroscopy

Extreme UltraViolet (EUV) spectroscopy measures the impurities inside the plasma core at the mid plane [12]. A comparison between shot #59 101 (dX = 100 mm), #59 115 (dX = 120 mm) and #59 438 (done after the cleaning session) is presented on Fig. 12.

During the two shots with plasma on the deposit, the W impurities measured inside the plasma are much stronger in comparison with a shot with a plasma far from the deposit. Putting the plasma directly on the deposit could lead to more erosion of the W-deposit and increase

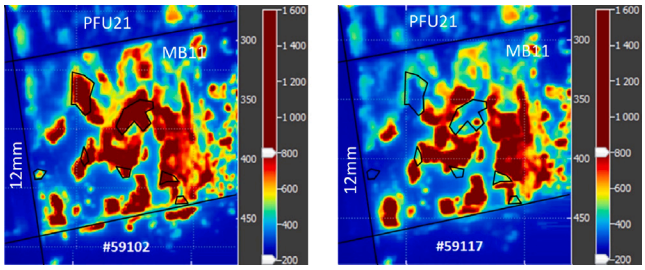

Fig. 11. Comparison of IR images with the VHR IR camera for shot #59 102 (left) and #59 117 (right).

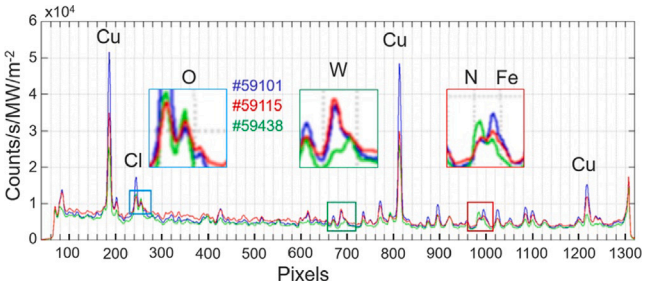

Fig. 12. UV spectroscopy measuring impurities inside plasma core. Comparison between shot #59 101 (blue), #59 115 (red) and #59 438 (green). (For interpretation of the references to color in this figure legend, the reader is referred to the web version of this article.)

the W going inside the plasma core. It was expected to see a decrease of Nitrogen (N) and Oxygen (O) during the cleaning session, the high temperature of the deposit would lead to degas impurities. Unfortunately, *N* and O inside the plasma core has not change between the beginning and the end of the cleaning session and was even stronger during the session after the cleaning session (shot #59 438). This was not expected but could be cause by the magnetic configuration of the shot #59 438, closer to the outer limiter with PFCs made of BN at the mid plane, leading to more *N* and O released inside the plasma. Other impurities like Copper (Cu), Chlorine (Cl) and Iron (Fe) are present since the beginning of the campaign and are slowly extracted outside of the tokamak during the campaign. The decrease shown is due to normal conditioning and no effect was expected by the experiments.

4.3.2. Visible spectroscopy

Visible spectroscopy, looking at the inner lower divertor, can measure impurities created on different specific locations. The brightnesses measured are converted into flux of particles taking into account the electron temperature and density estimated from the Langmuir probes [13]. On Fig. 13, the W ions flux profile on the lower divertor is presented for different shots of the session and compared with shot done before the cleaning session with the ISL far from the deposit (#59 037). During the cleaning session, with ISL on the deposit, the peak of flux is located around MB8 (for ISL on MB11) and reaches comparable values to scenarios with ISL far from the deposit (peak of flux on MB11-12 for ISL on MB16) with a flux of 2.5e19 ions/m2/s, except for the shot #59 117 which showed a larger peak of W ions flux (around 4e19 ions/m2/s). The peak of flux is shifted compared to the ISL. This may be due to perturbations and perpendicular drifts on the inner side. Moreover, the diagnostic lacks of spatial resolution between MB8 and MB11. Some probes on the MB11 (close to the MB10) may be inaccurate, explaining the large difference of ions flux between both sides of MB11.

On Fig. 14 is shown the peak ions flux of Boron (B), Carbon (C), N, O and W for the same shots. The peak ions fluxes are located at the same location as the W ones presented on Fig. 13 (so MB11 for

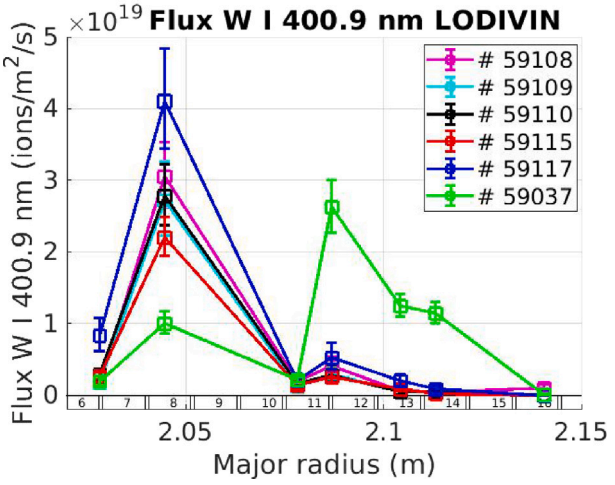

Fig. 13. W impurity flux.

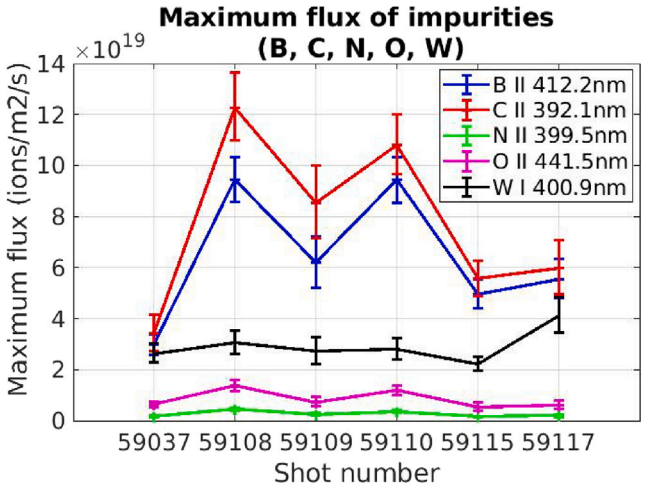

Fig. 14. Maximum flux for B, C, N, O and W impurities.

the shot #59 037 and MB8 for the other shots). The W impurities are generated along with the light impurities, explaining why the peak of each impurity is located from the same MB. The impurities coming from the deposit are much stronger when the ISL is on the deposit, in particular for the B (6.2e19 to 9.5e19 ions/m2/s for #58 108-#58 110 compared to 3e19 ions/m2/s for #59 037) and C (8.5e19 to 12e19 ions/m2/s for #58 108-#58 110 compared to 3.5e19 ions/m2/s for #59 037). The last two shots of the session (#59 115 and #59 117) show twice less flux of impurities compared to the beginning of the session (#58 108) for all light impurities, probably showing a small effect of cleaning during the session. Only the W was stronger. The peaked intensity of B and C are always stronger compared to the shot #59 037, while for *N* and O, the peaked intensity reached at the end of the session is comparable to the one for the shot #59 037.

4.4. Conclusion of the cleaning by the plasma

No clear effect of cleaning was seen by this experimental session with the ISL on the deposit, even if some results from the spectroscopy show a different generation of impurities when the deposit is heated by the plasma. But this experimental session was performed with a relatively cleaned lower divertor (after using the adhesive tape), reducing the possibility of generating UFOs and removing the deposit. This session has to be repeated on a dirtier lower divertor to see if the weakly adhered parts of the deposit could be removed by the plasma. This would lead to different results on the visible and EUV spectroscopy with more W and light impurities. A strike point sweeping needs also to be tested, in order to increase the thermal stress created on the deposit by cycling heating/cooling. The thermal expansion/compression involved could help to detach the deposit.

5. Conclusion

After a high fluence campaign when the same shot was repeated and cumulated 3 h of plasma, a W-deposit layer appeared, mostly on the HFS of WEST lower divertor, few cm away from the ISL. The growing of the deposit was monitored thanks to IR camera and shows a particular increase of the deposit area at the end of the campaign. The area particularly increased in the last hour of plasma, doubling its area covered on IR images. As this W-deposit hampered the operation when flakes of the deposit enters inside the plasma core, leading to radiative collapse, a cleaning of the lower divertor is needed to get rid of this. A first cleaning was performed during the shutdown between two campaigns by removing the weakly adhered parts of the deposit by using adhesive tape. This method was chosen because it can be performed inside the tokamak without generating dust. The efficiency of the cleaning was measured by confocal microscopy, showing that some localized high height weakly stuck deposit could be removed, but a large part of the deposit still remains stuck to the W-monoblock, with an average removed deposit thickness of 3.2 μm. An experiment was conducted during WEST C9 campaign to clean the deposit with the plasma, by putting the ISL directly on the deposit. The deposit was heated up to 1500 °C, but the cleaning effect was not significant. Spectroscopy measurement showed more impurities inside the plasma core (W) and from the deposit location (B,C,N,O) when the ISL is on the deposit compared to a pulse with usual ISL on MB15-MB16.

New ways to clean the lower divertor more efficiently need to be investigated, in particular using laser beams to sublimate the deposit [14].

CRediT authorship contribution statement

J. Gerardin: Writing – original draft, Software, Methodology, Investigation, Data curation. **Y. Corre:** Writing – review & editing, Supervision. **C. Desgranges:** Writing – review & editing, Software, Investigation, Formal analysis. **M. Diez:** Writing – review & editing, Software, Methodology, Investigation. **L. Dubus:** Software. **M. Firdaouss:** Writing – review & editing, Methodology. **J. Gaspar:** Writing – review & editing, Methodology, Investigation. **A. Grosjean:** Writing – review & editing, Validation, Software, Methodology, Investigation. **C. Guillemaut:** Software, Methodology. **C. Hernandez:** Methodology. **A. Huart:** Software. **H. Roche:** Software, Methodology. **S. Vives:** Writing – review & editing, Supervision, Resources.

Declaration of competing interest

The authors declare that they have no known competing financial interests or personal relationships that could have appeared to influence the work reported in this paper.

Data availability

Data will be made available on request.

References

[1] M. Missirlian, et al., The WEST project: Current status of the ITER-like tungsten divertor, Fusion Eng. Des. 89 (7) (2014) 1048–1053, http://dx.doi.org/10.1016/j.fusengdes.2014.01.050.

[2] E. Tsitrone, et al., Overview of plasma wall interactions in the first high particle fluence campaign of WEST, in: 26th PSI, France, 2024.

[3] A. Polevoi, et al., PFPO plasma scenarios for exploration of long pulse operation in ITER, Nucl. Fusion 63 (2023) 076003, http://dx.doi.org/10.1088/1741-4326/acd06f.

[4] C. Martin, et al., Post-mortem analysis of the deposit layers on the lower divertor after the high particle fluence campaign of WEST, Nucl. Mater. Energy 41 (2024) 101764, http://dx.doi.org/10.1016/j.nme.2024.101764.

[5] A. Widdowson, et al., Deposition of impurity metals during campaigns with the JET ITER-like Wall, Nucl. Mater. Energy 19 (2019) 218–224, http://dx.doi.org/10.1016/j.nme.2018.12.024.

[6] Y. Corre, et al., Visualisation of the deposited layer on the Toroidal Pumped Limiter of Tore Supra using IR data during disruptions, in: 32th EPS Conference on Controlled Fusion and Plasma Physics, France.

[7] J. Gaspar, et al., Thermal and statistical analysis of the high-Z tungsten-based UFOs observed during the deuterium high fluence campaign of the WEST tokamak, Nucl. Mater. Energy 41 (2024) 101745, http://dx.doi.org/10.1016/j.nme.2024.101745.

[8] X. Courtois, et al., Full coverage infrared thermography diagnostic for WEST machine protection, Fusion Eng. Des. 146 (2019) 2015–2020, http://dx.doi.org/10.1016/j.fusengdes.2019.03.090.

[9] J. Gaspar, et al., Overview of the emissivity measurements performed in WEST : in situ and post-mortem observations, Nucl. Fusion 62 (9) (2022) 096023, http://dx.doi.org/10.1088/1741-4326/ac6f68.

[10] J. Gaspar, et al., In-situ estimation of the thermal resistance of carbon deposits in the JET tokamak, Int. J. Therm. Sci. 104 (2016) 292–303, http://dx.doi.org/10.1016/j.ijthermalsci.2016.01.022.

[11] M. Houry, et al., The Very High spatial Resolution infrared thermography on ITER-like tungsten monoblocks in WEST Tokamak, Fusion Eng. Des. 146 (2019) 1104–1107, http://dx.doi.org/10.1016/j.fusengdes.2019.02.017.

[12] R. Guirlet, et al., Extreme UV spectroscopy measurements and analysis for tungsten density studies in the WEST tokamak, Plasma Phys. Control. Fusion 64 (10) (2022) 105024, http://dx.doi.org/10.1088/1361-6587/ac8d2c.

[13] A. Grosjean, et al., Development of an integrated multidiagnostic to assess the high-Z impurity fluxes in the metallic environment of WEST using IMAS, IEEE Trans. Plasma Sci. 50 (11) (2022) 4251–4256, http://dx.doi.org/10.1109/TPS.2022.3187619.

[14] G. Zhu, et al., Mechanism and application of laser cleaning: A review, Opt. Lasers Eng. 157 (2022) 107130, http://dx.doi.org/10.1016/j.optlaseng.2022.107130.